HHS Public Access

Author manuscript

Nat Neurosci. Author manuscript; available in PMC 2015 January 01.

Published in final edited form as:

Nat Neurosci. 2014 July ; 17(7): 943–952. doi:10.1038/nn.3732.

ALK5-dependent TGF-β signaling is a major determinant of late stage adult neurogenesis

Yingbo He[1], **Hui Zhang**[1], **Andrea Yung**[1], **Saul A Villeda**[1], **Philipp A Jaeger**[1], **Oluwatobi Olayiwola**[1], **Nina Fainberg**[1], and **Tony Wyss-Coray**[1,2,*]

[1]Department of Neurology and Neurological Sciences, Stanford University School of Medicine, Stanford, California 94305, USA

[2]Center for Tissue Regeneration, Repair and Rehabilitation, VA Palo Alto Health Care System, Palo Alto, California 94304, USA

Abstract

The transforming growth factor-β (TGF-β) signaling pathway serves critical functions in central nervous system (CNS) development, but apart from its proposed neuroprotective actions, its physiological role in the adult brain is unclear. We observed a prominent activation of TGF-β signaling in the adult dentate gyrus and expression of downstream Smad proteins in this neurogenic zone. Consistent with a function of TGF-β signaling in adult neurogenesis, genetic deletion of the TGF-β receptor ALK5 reduced the number, migration, and dendritic arborization of newborn neurons. Conversely, constitutive activation of neuronal ALK5 in forebrain caused a striking increase in these aspects of neurogenesis and was associated with higher expression of c-fos in newborn neurons and with stronger memory function. Our findings describe a new and unexpected role for ALK5-dependent TGF-β signaling as a regulator of the late stages of adult hippocampal neurogenesis which may have implications for changes in neurogenesis during aging and disease.

Introduction

TGF-β superfamily members, including TGF-βs, bone morphogenic proteins (BMP)s, growth and differentiation factors (GDFs), activins, and nodal control critical aspects of brain development, and a growing literature suggests that they fulfill important functions in the adult brain as well[1]. The founding members of this family, TGF-β1, 2 and 3, are dimeric polypeptide growth factors[2] which are broadly expressed in the brain[3]. Canonical TGF-β

*Correspondence: twc@stanford.edu. Tel: (650) 852 3220 Fax: (650) 849 0434.

Author Contributions

Y.H. contributed to all aspects of experiments and data analysis; H.Z. generated the *ALK5*^{CA} mouse; A.Y. assisted with *ALK5* shRNA experiments and *in vivo* data analysis; P.A.J. assisted with microarray data analysis; S.A.V. assisted with contextual fear conditioning experiments; O.O. assisted with doxycycline experiments; N.F. assisted with Y maze experiments; Y.H. and T.W.-C. wrote the manuscript; T.W.-C. supervised the project.

Accession codes

Gene Expression Omnibus: GSE53761.

signaling is initiated by ligand binding to a high-affinity transmembrane TGF-β type II receptor (TβRII), which subsequently phosphorylates TGF-β type I receptor activin-like kinase 5 (TβRI or ALK5)[4]. This leads to phosphorylation of Smad2 and Smad3 proteins, which form a heteromeric complex with Smad4 and translocate into the nucleus where they regulate transcription[4]. TGF-βs can also activate other signaling cascades in a context-dependent manner, such as MAPK, JNK, and PKC pathways[5].

TGF-β type I receptor ALK5 is highly expressed in migrating neurons of the developing cortex[6] and TGF-β signaling regulates self-renewal of neural stem cells in the developing midbrain[7]. TGF-βs have also been shown to promote the sprouting and elongation of neurites in dissociated hippocampal cultures[8] and to regulate synaptic growth in *Drosophila* depending on TGF-β type I receptor[9]. Moreover, TGF-β signaling was reported to mediate axon specification during brain development[10]. In the adult brain TGF-βs seem to have broad neuroprotective functions[11]. They are induced in response to injury and have thus been implicated in neurodegenerative diseases[12]. For example, deficiency in TGF-β1 results in synapto-dendritic degeneration and increased susceptibility to excitotoxic injury[13], and reduced expression of TβRII in neurons promotes neurodegeneration in a mouse model of Alzheimer's disease[14].

Consistent with its function in regulating developmental neurogenesis, TGF-β1 can reduce adult neurogenesis by inhibiting cell cycle progression in neural progenitor cells and promoting stem cell quiescence[15, 16]. Adult neurogenesis persists in the subventricular zone of the lateral ventricles and the subgranular zone of the hippocampal dentate gyrus; the latter process exerts an important role in hippocampus-dependent learning, memory, and other cognitive functions[17]. Neurogenesis in the adult brain is regulated through a number of signaling pathways[18] and in response to physiological stimuli such as aging, exercise, and CNS injury[19]. Many of these factors regulate early events of neurogenesis, including quiescence, proliferation, and fate specification of neural stem cells[20] but relatively little is known about factors that regulate the subsequent survival, maturation, and functional integration of newborn neurons.

Here we demonstrate that TGF-β signaling serves a critical role in late stage adult neurogenesis. We observed that Smad2/3-dependent signaling is prominently activated in dentate gyrus postmitotic immature neurons and adult mature neurons but not in radial glia-like stem cells or neural progenitor cells. Genetic knockdown of TGF-β type I receptor ALK5 in proliferating progenitors in the dentate gyrus resulted in reduced survival, migration, and shorter dendrite length of newborn neurons, while activation of this receptor in transgenic mice had the opposite effects and improved hippocampus-dependent working and spatial memory. Our findings demonstrate that TGF-β signaling through ALK5 is necessary and sufficient to maintain late events during adult hippocampal neurogenesis.

Results

Canonical TGF-β signaling is active in the dentate gyrus

We had reported earlier that within the mouse brain TGF-β signaling is highest in the hippocampus[21]. To explore this further, we dissected brains of previously described

unmanipulated Smad binding elements (SBE)-luciferase reporter mice[22] into different brain regions. In these mice, luciferase is expressed under the SBE promoter and its activity is positively correlated with TGF-β signaling. We found highest luciferase activity in the adult dentate gyrus, lower signals in the *Cornu Ammonis* (CA) area of the hippocampus, and no signal in the cerebellum or in non-transgenic littermate control mice (Fig. 1a). Immunohistochemical staining of the adult dentate gyrus showed that under physiological conditions, p-Smad2, downstream of TGF-β signaling was prominently expressed in the granule zone of the dentate gyrus (Fig. 1b). More than 95% of p-Smad2+ cells expressed NeuN (mature neuron marker) (Fig. 1b,c). In contrast, few Sox2+GFAP+ radial glia-like cells, MCM2+ or Tbr2+ neural progenitor cells in the dentate gyrus showed detectable p-Smad2 immunoreactivity (Fig. 1b,c). Interestingly, almost 5% of p-Smad2+ cells expressed doublecortin (DCX, neuroblast and immature neuron marker) (Fig. 1b,c). DCX expressing cells are highly heterogeneous and can be divided into proliferating neuroblasts and postmitotic immature neurons according to their proliferative activity[23]. By using proliferating cell nuclear antigen (PCNA) as a proliferation marker, we found greater than 95% of p-Smad2+DCX+ cells were negative for PCNA but exhibited neurites (Fig. 1b), indicating they are postmitotic immature neurons. Furthermore, we quantified p-Smad2+ and p-Smad2– cell populations in individual cell types of the neuronal lineage in the dentate gyrus. More than 90% of postmitotic immature neurons and 98% of mature neurons expressed p-Smad2 while only few Sox2+GFAP+ cells, MCM2+ cells, Tbr2+ cells, and DCX+PCNA+ cells were positive for p-Smad2 (Fig. 1d). Thus, we conclude that endogenous TGF-β signaling is active in postmitotic immature neurons and mature neurons of the dentate gyrus.

ALK5 is required for adult neurogenesis *in vivo*

TGF-β type I receptor ALK5 mediates signaling of TGF-βs and GDF8, GDF9, and GDF11[24]. Among them, GDF11 regulates neurogenesis in olfactory development through ALK5[25]. Because TGF-β signaling is active in postmitotic immature and mature neurons of the dentate gyrus (Fig. 1b), we hypothesized TGF-β signaling through ALK5 may have a role in late stages of adult hippocampal neurogenesis as well. To test this hypothesis, we generated conditional knockout mice for ALK5 (*ALK5*^{cKO}) by crossing homozygous ALK5-floxed mice (*ALK5*^{flox}) with *CamKII*α-*cre* transgenic mice (Supplementary Fig. 1a), leading to a 70% reduction of hippocampal ALK5 protein expression (Supplementary Fig. 1b,c) and an approximate 20% decrease of Smad2 signaling in the dentate gyrus (Supplementary Fig. 1d,e). The differences in reduction could be due to difficulties in quantifying actual downstream activity of ALK5 as a function of p-Smad2 and to compensatory increases in TGF-β signaling after deleting ALK5.

To assess the usefulness of the *CamKII*α promotor for our studies, we tracked *CamKII*α-driven gene expression *in vivo* by crossing *CamKII*α-*cre* transgenic mice with ROSA26-Actin promoter-loxP-mT-pA-loxP-mEGFP-pA reporter mice (herein called *mT/mG* mice)[26]. In double transgenic mice, cre-induced recombination in CamKIIα expressing cells led to excision of the gene encoding for membrane targeted tandem dimer Tomato (mT) and a transcriptional stop sequence, resulting in the expression of membrane-targeted enhanced green fluorescent protein (eGFP, mG) (Supplementary Fig. 1f). As a control, *mT/mG*

reporter mice lacking cre recombinase expressed only mT but not mG (Supplementary Fig. 1f). Furthermore, we used a set of developmental markers of the neuronal lineage to identify different cell types expressing eGFP in the dentate gyrus. More than 95% of eGFP+ cells in the dentate gyrus expressed NeuN while most of the remaining cells expressed DCX and lacked PCNA (Supplementary Fig. 1f,g). We detected very few eGFP+ cells expressing either Sox2 plus GFAP, MCM2, or Tbr2 (Supplementary Fig. 1f,g). We further quantified eGFP+ and eGFP– cell populations in individual cell types of the neuronal lineage in the dentate gyrus. More than 90% of NeuN+ neurons and almost 60% of DCX+PCNA– postmitotic immature neurons expressed eGFP, while fewer than 5% of other cell types were eGFP+ (Supplementary Fig. 1h). These results are in line with previous reports[27, 28, 29] and demonstrate that the *CamKII*α promoter is activated late during neuronal development resulting in expression of downstream transgenes in postmitotic immature neurons in the granule cell layer (GCL) and in most mature neurons in the forebrain. Importantly, this transgene expression pattern largely mimics the endogenous pattern of p-Smad2 expression and makes *ALK5*^{cKO} mice a useful model to study the necessity of TGF-β signaling in the adult brain.

Consistent with this expression pattern, reduction of ALK5 in *ALK5*^{cKO} mice did not alter the number of Sox2+ neural stem cells compared with *ALK5*^{flox} mice (Supplementary Fig. 2a,b), however, it resulted in a more than 30% reduction in the number of DCX+ newborn neurons (Fig. 2a,b). To determine whether the decrease in DCX+ neurons in *ALK5*^{cKO} mice was the result of reduced production of committed neurons, the thymidine analog Bromodeoxyuridine (BrdU) was injected into mice for 6 days and the number of committed neurons was evaluated 1 day later. The percentage of BrdU+DCX+ cells was the same between *ALK5*^{flox} and *ALK5*^{cKO} mice, indicating that ALK5 is not affecting the production of committed neurons from progenitors (Supplementary Fig. 2c). In addition, both groups of mice had equivalent overall numbers of proliferating cells and proliferating neuroblasts in the dentate gyrus, based on independent immunohistochemical assessment of PCNA and DCX (Supplementary Fig. 2d,e). To determine if the number of DCX+ cells is reduced in *ALK5*^{cKO} mice because the immature neurons mature at greater numbers into neurons, we birth-dated newly born neurons by injecting BrdU daily into adult *ALK5*^{flox} and *ALK5*^{cKO} littermates for 6 days and analyzed their brains 28 days later. *ALK5*^{cKO} mice had about 20% fewer BrdU+NeuN+ cells in the dentate gyrus than *ALK5*^{flox} mice (Fig. 2c) suggesting that lack of ALK5 in forebrain neurons reduces the survival of DCX+ cells.

To further ascertain that loss of ALK5 reduces neurogenesis and to rule out confounding effects of chronic reduction of ALK5, we developed a lentivirus (LV)-mediated knockout technique to acutely reduce ALK5 expression in CamKIIα-expressing cells (Supplementary Fig. 3a). *ALK5*^{flox} mice were stereotaxically injected into the dentate gyrus in one hemisphere with virus encoding for *cre* recombinase and *eGFP* under control of the *CamKII*α promoter (LV-*cre-eGFP*) or with virus encoding for *eGFP* only (LV-*eGFP*) into the contralateral dentate gyrus (Fig. 2d). LV-*cre-eGFP* significantly decreased p-Smad2 expression in infected cells in the dentate gyrus of *ALK5*^{flox} mice (Supplementary Fig. 3c,d). Consistent with the results from *CamKII*α-*cre* transgenic mice, out of the roughly 30% infected cells in the dentate gyrus (Supplementary Fig. 3b), the vast majority of eGFP

expressing cells were NeuN+ while the rest were DCX+, PCNA–. We did not detect infected, eGFP positive cells expressing Sox2 plus GFAP, MCM2, or Tbr2 (Supplementary Fig. 3e). Dividing cells were labeled with BrdU for 6 consecutive days and brains were analyzed 28 days later (Fig. 2d). Consistent with data above with stable knockdown of ALK5, the percentage of BrdU+NeuN+ cells was significantly decreased (Fig. 2e) and the total number of DCX+ cells was around 22% lower (Fig. 2f,g) in the LV-*cre-eGFP* injected dentate gyrus compared with the LV-*eGFP* injected side Furthermore, we counted the number of eGFP+DCX+ cells at 6, 14, and 21 days post injection (dpi) and found significantly reduced cell numbers at 21 dpi in the LV-*cre-eGFP*-injected dentate gyrus compared with that on the contralateral side (Supplementary Fig. 3f). Together, these findings show that ALK5 is necessary to maintain wildtype levels of neurogenesis in the dentate gyrus.

ALK5 is required for the development of immature neurons

The above experiments reduced ALK5 expression in immature and mature neurons and raise the question whether ALK5 regulates neurogenesis in a cell-autonomous way in immature neurons or indirectly through mature neurons. We thus engineered retroviral vectors to directly infect and manipulate individual dividing newborn cells in the adult mouse dentate gyrus, coexpressing eGFP and either short-hairpin RNAs (shRNAs) targeting *ALK5* (shRNA-A1 and shRNA-A2) or scrambled control shRNAs (shRNA-C) (Supplementary Fig. 4a). We injected shRNA-A1, which effectively knocked down ALK5 and p-Smad2 (Supplementary Fig. 4b-e) into one side of the dentate gyrus and shRNA-C as a control into the contralateral side of 2-month-old C57BL/6 mice to infect proliferating neuronal progenitor cells *in vivo* (Fig. 3a). Remarkably, the number of eGFP+DCX+ infected newborn neurons in the shRNA-A1-injected dentate gyrus was reduced by almost 80% at 14 dpi compared with the shRNA-C contralateral side after normalizing to the cell number at 7 dpi (Fig. 3b). This reduction was confirmed by co-injection of a mixture of retroviruses encoding for shRNA-A1 and *mCherry* into both sides of the dentate gyrus (Supplementary Fig. 4a), resulting in cells expressing either eGFP shRNA-A1 alone, mCherry alone, or both markers together. The number of cells in the dentate gyrus receiving ALK5 knockdown virus (eGFP+ and eGFP+mCherry+) was reduced again by more than 60% at 14 dpi and continued to decrease by 21 dpi compared with cells receiving the control virus (mCherry+) alone after normalizing to the number at 7 dpi (Supplementary Fig. 4f). This progressive depletion of newborn cells is consistent with the finding above that ALK5 is required for the survival of newborn neurons, and suggests that ALK5 acts, at least in part, in a cell-autonomous manner.

It was striking that the remaining *ALK5* shRNA-A1 expressing DCX+ cells had very short processes (Fig. 3c,d), which prompted us to assess their morphology in more detail. Indeed, while shRNA-C-infected cells showed a polarized morphology with a single apical branch into the GCL at 7 dpi, shRNA-A1-infected immature neurons displayed on average 70% shorter apical branches and many cells had no dendrites at all (Fig. 3e). These shorter branches were still apparent at 14 dpi and were accompanied by less elaborated dendrites (Fig. 3f,g). Moreover, at 14 dpi, almost 50% of shRNA-C-infected immature neurons, but only around 20% of shRNA-A1-infected neurons, migrated into the GCL (Fig. 3h). Delayed

dendritic development of immature neurons was also observed in mice injected with shRNA-A2 (Supplementary Fig. 5). In summary, knockdown of ALK5 decelerated survival, migration, and dendritic development of newborn neurons. While some of these effects of ALK5 appear to be cell-autonomous, we cannot exclude non-autonomous effects, e.g. as a result of changes in paracrine signals produced by more mature, transgene expressing neurons within the neurogenic niche.

Transgenic activation of ALK5 in the dentate gyrus

Having shown that ALK5-dependent TGF-β signaling is necessary for the normal survival and maturation of immature neurons in the adult brain, we asked if increased ALK5 signaling may be sufficient to increase neurogenesis. This question is significant because canonical TGF-β signaling is constitutively active in the hippocampus and increases in response to injury[21]; in addition, TGF-β signaling induced by injury is accompanied by increased neurogenesis[30]. To better understand the effects of TGF-β signaling during the late stages of neurogenesis, we generated *ALK5*^{CA} mice by crossing *CamKII*α-*tTA* and tetO-*ALK5*^{CA} mice (Supplementary Fig. 6a). In *ALK5*^{CA} mice, a constitutively active *ALK5* transgene (*ALK5*^{CA}) and a reporter eGFP are expressed under a *CamKII*α promoter driving expression in forebrain neurons. Littermates, which did not express tTA but only tetO-ALK5^{CA} were used as controls and are referred to as *ALK5*^{Ctrl} mice. As expected, *ALK5*^{CA} induced canonical TGF-β signaling in the absence of TGF-β ligands *in vivo*, as demonstrated by p-Smad2 expression (Supplementary Fig. 6b), and could be regulated by doxycycline *in vivo* (Supplementary Fig. 6c). No expression of eGFP was observed in *ALK5*^{Ctrl} mice, indicating that the tetO promoter was not leaking in the absence of tTA (Supplementary Fig. 6d).

To validate that eGFP can be used as a reporter of ALK5^{CA} from the bi-directional promoter *in vivo*, we quantified eGFP and a hemagglutinin (HA) tag, which had been engineered into the N-terminus of the *ALK5*^{CA} coding sequence (Supplementary Fig. 6a), using immunoblot and fluorescent immunostaining. More than 95% of eGFP+ cells expressed HA demonstrating similar bidirectional expression levels of eGFP and HA, and by inference, of ALK5^{CA} (Supplementary Fig. 6c). Using eGFP or HA as surrogate markers for *ALK5*^{CA} transgene expression, we found about 40% of NeuN+ cells and roughly 30% of DCX+ cells in the dentate gyrus expressed eGFP/HA (Supplementary Fig. 6e). Importantly, eGFP was only expressed in mature neurons, indicated by NeuN labeling, and in postmitotic immature neurons, indicated by eGFP, DCX, and PCNA triple labeling (Supplementary Fig. 6f). In contrast, we were unable to find eGFP expression in Sox2+GFAP+ cells, MCM2+ cells, or Tbr2+ cells in the subgranular zone (SGZ) (Supplementary Fig. 6f). Cumulatively, these results again demonstrate that CamKIIα-driven genes are expressed in postmitotic immature neurons and mature neurons in the dentate gyrus, which largely mimics the endogenous pattern of p-Smad2 expression (Supplementary Fig. 6g). These mice should thus allow us to assess the effects of increased TGF-β signaling in forebrain neurons during the late stages of neuronal development in the adult hippocampus in a physiologically relevant fashion.

ALK5^{CA} mice show increased hippocampal neurogenesis

To assess the effect of increased ALK5 activity on the late stages of neurogenesis, we analyzed brains from 3-month-old *ALK5*^{CA} transgenic mice and *ALK5*^{Ctrl} littermates. We found that *ALK5*^{CA} mice had an almost 60% increase in the number of DCX+ cells in the dentate GCL and SGZ compared with *ALK5*^{Ctrl} mice, while no differences were detected in the number of Sox2+ neural stem cells (Fig. 4a,b and Supplementary Fig. 7a). To dissect the effects of activated TGF-β signaling on newborn neurons in the dentate gyrus, we treated *ALK5*^{CA} and *ALK5*^{Ctrl} mice with BrdU daily for 6 days and different groups of mice were then sacrificed either 1 day (short term) or 28 days (long term) later (Supplementary Fig. 7b). In the short-term group, the total number of BrdU+ cells was unchanged between transgenic and control mice (Supplementary Fig. 7c). Similarly, we could not detect an increase in the fraction of newly committed immature neurons (BrdU+DCX+) in *ALK5*^{CA} mice (Supplementary Fig. 7c), which suggests that cell proliferation and neuronal commitment was not altered by activated TGF-β signaling. In contrast, in the long-term group, the overall number of BrdU labeled cells was almost three times higher in *ALK5*^{CA} mice than in *ALK5*^{Ctrl} mice (Fig. 4c,d). Among the BrdU+ cells, the fraction of NeuN+BrdU + newborn granule neurons was significantly higher in *ALK5*^{CA} compared with *ALK5*^{Ctrl} mice (Fig. 4d). This increase in cell number did not result in larger or heavier brains (data not shown). To determine how ALK5 may increase survival of neurons we assessed the number of cells undergoing apoptosis based on nuclear morphology and showing features of pyknosis (Supplementary Fig. 7d). *ALK5*^{CA} mice displayed three times fewer apoptotic cells in the SGZ than *ALK5*^{Ctrl} mice (Fig. 4e). Consistent with this observation, hippocampi from *ALK5*^{CA} mice showed above two times more anti-apoptotic protein Bcl-2 and 70% less pro-apoptotic protein Bax than those from ALK5^{Ctrl} mice by western blot (Fig. 4f,g and Supplementary Fig. 7e). Together, these data suggest that increased TGF-β signaling in the forebrain of *ALK5*^{CA} mice promotes newborn neuron survival by antagonizing apoptotic pathways.

To confirm that this increase in newborn neuron survival was indeed the result of activated ALK5 signaling in the adult, we took advantage of the regulatable nature of the *ALK5*^{CA} transgene and reversed TGF-β signaling to normal levels by doxycycline (Fig. 4h). Mice were raised with doxycycline from E17 until P56, when half of them were switched to either regular diet or kept on doxycycline-containing feed. One month later, all mice were given BrdU for 6 days and sacrificed 28 days later. As expected, doxycycline treatment of *ALK5*^{CA} mice abolished the expression of both eGFP and HA (Supplementary Fig. 6c), and by inference, of ALK5^{CA}. Indeed, doxycycline treatment reversed the effects of activated ALK5 signaling in *ALK5*^{CA} mice by reducing the number of DCX+ newborn neurons in *ALK5*^{CA} mouse dentate gyrus with a strong trend (Fig. 4i). Importantly, doxycycline treatment also significantly decreased the overall number of BrdU+ cells in the dentate gyrus of *ALK5*^{CA} mice to levels comparable with those in control mice (Fig. 4j). In addition, we observed a trend towards an increased fraction of BrdU+NeuN+ cells in sham treated *ALK5*^{CA} mice and a reversal following drug treatment (Supplementary Fig. 7f). Overall, our data demonstrate that increased TGF-β signaling in forebrain neurons promotes adult hippocampal neurogenesis by increasing the survival of adult newborn neurons.

Activation of ALK5 enhances maturation of newborn neurons

ALK5^{CA} mice exhibited a prominent difference in the relative position of both DCX+ cells and BrdU+ cells within the GCL compared with *ALK5*^{Ctrl} littermates (Fig. 4a,c). To characterize these changes, we stained brain sections from *ALK5*^{CA} and control littermates with DCX and the nuclear dye Topro-3 to label new neurons within the cellular layer of the dentate gyrus (Fig. 5a). We found more than 90% of DCX+ neurons were localized within the inner third of the GCL in *ALK5*^{Ctrl} mice, consistent with previous reports[31] (Fig. 5b). In stark contrast, more than 30% of these immature neurons in *ALK5*^{CA} mice migrated into the middle and outer thirds of the GCL, with a few cells even migrating into the molecular layer (Fig. 5b). In support of a transgene specific effect, this accelerated migration of newborn neurons in *ALK5*^{CA} mouse dentate gyrus was suppressed by doxycycline treatment (Supplementary Fig. 8a,b). To determine if these effects are cell-autonomous or not, we took advantage of the eGFP reporter in *ALK5*^{CA} mice and measured the distribution of transgenic eGFP+DCX+ cells and non-transgenic eGFP–DCX+ cells in the dentate gyrus separately. Unexpectedly, both of these cell types in *ALK5*^{CA} mice migrated further into the GCL than DCX+ cells in *ALK5*^{Ctrl} mice, although more eGFP+DCX+ cells migrated into the middle layer of the GCL than eGFP–DCX+ cells of *ALK5*^{CA} mice (Fig. 5b). Thus, in addition to increasing the overall number of newborn neurons in the dentate gyrus, activated TGF-β signaling in the forebrain promotes neuronal migration into the GCL and beyond, and this effect appears to be largely cell non-autonomous.

Besides migration, the morphology of DCX+ cells in *ALK5*^{CA} mice was strikingly different from that in *ALK5*^{Ctrl} littermates (Fig. 4a). To characterize these changes, we quantified cellular morphology by reconstructing dendritic arborization and branching of individual DCX+ neurons using confocal microscopy and digital imaging software (Fig. 5c). Both eGFP+DCX+ and eGFP–DCX+ cells in *ALK5*^{CA} mice displayed a greater number of elaborated dendrites and stubby arbors compared with those in *ALK5*^{Ctrl} mice, as indicated by significant increases in both dendritic number and length (Fig. 5d,e). These two types of DCX+ cells in *ALK5*^{CA} mice demonstrated also larger cell bodies indicative of hypertrophy (Fig. 5f) and an increase in the dendritic complexity as assayed by Sholl analysis (Fig. 5g) . This enhanced dendritic development of DCX labeled neurons in *ALK5*^{CA} mice was again reversed by doxycycline treatment (Supplementary Fig. 8a,c,d). These results imply that ALK5-dependent TGF-β signaling promotes maturation of newborn neurons in the adult hippocampus by accelerating their dendritic and soma development and that these effects on newborn neurons are largely non-autonomous.

Activation of ALK5 induces changes in gene expression

To gain insight into the molecular mechanism by which ALK5 signaling regulates adult neurogenesis, we measured global gene expression in hippocampi of *ALK5*^{CA} and *ALK5*^{Ctrl} mice using gene microarray analysis (Fig. 6a and Supplementary Table 1). The top 27 differentially expressed genes between the two groups of mice are involved in brain development ($P = 0.000452$), neuronal generation ($P = 0.0343$) and migration ($P = 0.0141$), synaptic transmission ($P = 0.0361$), cell death ($P = 0.00390$) and movement ($P = 0.000135$), cell cycle ($P = 0.00180$), and neurologic diseases($P = 0.0000529$), processes and functions that are in line with the effects on neurogenesis we describe in this study. For example, the

classical complement component *C1q* which mediates developmental elimination of synapses[32] was reduced in *ALK5*^{CA} mice, while T box brain 1 (*Tbr1*), an important regulator in cortical laminar organization and guidance of cortical axons[33], BTB (POZ) domain containing 6 (*Btbd6*), which is involved in late neuronal development[34], as well as ryanodine receptor (*Ryr*), a controller of calcium release and neuronal differentiation[35], were increased. Similarly increased in hippocampi of *ALK5*^{CA} mice were the kinesin family members kinesin light chain (*Klc1*), kinesin 2 (*Kns2*), and kinesin family member 1B (*Kif1b*), which are implicated in neuronal migration[36]. Additionally, Ingenuity network analysis generated two gene networks linked to MAPK pathways including the JNK (MAPK8) pathway and related proteins (Fig. 6b). To verify this pathway, we assessed phosphorylation of JNK (p-JNK) from dissected hippocampi of *ALK5*^{CA} and *ALK5*^{Ctrl} mice by western blot. Indeed hippocampi of *ALK5*^{CA} mice showed higher levels of p-JNK than *ALK5*^{Ctrl} mice (Fig. 6c), supporting the Ingenuity network analysis and implying a critical role of JNK signaling in ALK5-induced adult neurogenesis.

Activation of ALK5 enhances neuronal activity and memory

Since increased TGF-β signaling in *ALK5*^{CA} mice enhances the maturation as well as the overall number of newborn neurons, we reasoned that these mice may have greater numbers of active neurons. Changes in the expression of immediate-early genes such as c-fos are correlated with neuronal activation[37]. Interestingly, *ALK5*^{CA} mice showed a greater than twofold increase in c-fos immunoreactive cells in the dentate gyrus compared with *ALK5*^{Ctrl} mice (Fig. 7a,b). Moreover, this increase can be reversed to basal levels by doxycycline treatment (Fig. 7e) confirming the dependence on activated ALK5. To determine the fraction of newborn neurons expressing c-fos, *ALK5*^{CA} and *ALK5*^{Ctrl} mice were treated with BrdU, and c-fos expression in the dentate gyrus was quantified 28 days later by confocal microscopy. Indeed the percentage of c-fos expressing NeuN+BrdU+ cells was markedly increased in *ALK5*^{CA} compared with *ALK5*^{Ctrl} mice (Fig. 7c,d), indicating that more newborn neurons are active overall in the *ALK5*^{CA} mouse dentate gyrus.

Based on these findings, we investigated whether *ALK5*^{CA} mice might show behavioral changes. To this end, we measured hippocampus-dependent working memory in cohorts of *ALK5*^{CA} mice and littermate controls with a Y maze and spatial memory with a contextual fear conditioning paradigm. Interestingly, *ALK5*^{CA} mice made significantly more spontaneous alternations than any of the three control mouse groups (Fig. 7f) while making comparable numbers of arm entries overall (Supplementary Fig. 9a). Moreover, *ALK5*^{CA} mice displayed a stronger contextual freezing response than control mice (Fig. 7g) and showed no difference in cued freezing (Supplementary Fig. 9b), demonstrating increased hippocampus-dependent spatial memory. In aggregation, these findings demonstrate improved hippocampus-dependent behavioral function in *ALK5*^{CA} mice.

Discussion

Neurogenesis in the adult dentate gyrus is a multistep process dynamically regulated by a growing number of soluble signaling factors and pathways[18]. Identifying and understanding these cues may provide guidance for potential applications of neural stem and progenitor

cells in regenerative medicine. Here, we demonstrate that canonical TGF-β signaling is active in the late stages of adult neurogenesis, including in postmitotic immature and recently born mature neurons of the dentate gyrus under physiological conditions. Based on loss- and gain-of-function *in vivo* models, our data demonstrate that TGF-β signaling through ALK5 not only regulates survival, migration, and dendritic development of newborn neurons in the adult dentate gyrus but has a role in cognitive function as well.

TGF-β signaling has previously been implicated in embryonic neurogenesis. During development, it regulates self-renewal of neural stem cells[7] and promotes axon specification[10] in the brain. TGF-β1 also promotes the sprouting and elongation of neurites in cell culture[8]. Consistent with these findings, our current work demonstrates that neuronal TGF-β signaling positively regulates adult hippocampal neurogenesis in mice. In contrast, high levels of soluble TGF-β1 lead to a strong inhibition of neurogenesis in the dentate gyrus of transgenic mice overproducing TGF-β1 from astrocytes[15] or in the subventricular zone and dentate gyrus of rats infused with recombinant TGF-β1[16]. These, apparently contradicting, results between the current and previous studies are likely explained by the highly context-dependent effects of TGF-βs in general and the effect on different cell types in the neurogenic niche in particular. Thus, soluble and extracellular TGF-β1 has the capacity to activate signaling in any cell type in the neurogenic niche, and we showed previously that it inhibits proliferation of NPCs by blocking the cell cycle[15]. However, TGF-β signaling controlled by the *CamKII*α promoter in *ALK5*^{CA} mice or *ALK5*^{cKO} mice acts only on forebrain neurons or recently born brain cells committed to the neuronal lineage and thus mimics the signaling pattern of TGF-β signaling we observed in the adult dentate gyrus of wildtype mice. Future studies need to evaluate the role of cell-autonomous activation of TGF-β signaling in other cell types in the neurogenic niche. Also, because ALK5 can transduce signals by TGF-βs and some GDF family members[24], it is currently unclear which growth factor(s) are responsible for the observed physiological effects of ALK5.

During hippocampal neurogenesis, many progenitor cells are born but only a small fraction survives and integrates into the neuronal circuitry. TGF-β1 has neurotrophic properties in adult neurons and a previous study showed increased survival of cultured NPCs treated with TGF-β1[38]. In line with these data, we found that elevated TGF-β signaling in *ALK5*^{CA} mice promotes the survival of newborn neurons, whereas deficiency of ALK5 in *ALK5*^{cKO} mice or by lentivirus and retrovirus suppresses the survival of newborn neurons. Additionally, the neural stem cell pool and the proliferation of immature neurons were not affected. Different mechanisms have been proposed how TGF-β signaling may promote neuronal survival including by increasing the expression of Bcl-2[39] and inhibiting caspase-3 activation[13], by regulating Ca2+ homeostasis[39], or by increasing the production of other neurotrophic factors[40]. We counted fewer pyknotic cells in the SGZ of *ALK5*^{CA} mice compared with *ALK5*^{Ctrl} mice, and this reduction was accompanied by lower levels of pro-apoptotic protein Bax and higher levels of anti-apoptotic protein Bcl-2 in the hippocampus. These findings are in line with the notion that TGF-β signaling increases the survival of newborn neurons by reducing apoptosis.

Recent studies showed that TGF-β signaling is required for axon specification in the developing mouse brain[10] and earlier findings showed it can regulate arborization of

neurons in cell culture[8]. We used here a cell-type-specific, retrovirus-based strategy to characterize the requirement of TGF-β signaling in migration and dendritic development of adult hippocampal neurons. ALK5-deficient newborn granule cells in the dentate gyrus showed a striking decrease or delay in acquiring dendritic complexity, developing shorter and fewer dendrites. On the other hand, newly generated granule neurons in *ALK5*^{CA} mice with increased TGF-β signaling in the forebrain displayed a prominent increase in dendritic arborization and complexity. It is intriguing that newborn cells in *ALK5*^{CA} mice are also more active as documented by their expression of cfos, and surrounded by an increased number of c-fos expressing neurons in the dentate gyrus. In support of a connection between the increase in mature newborn neurons and their increased activity, we observed a significant improvement in hippocampus-dependent learning and memory tasks in *ALK5*^{CA} compared with *ALK5*^{Ctrl} mice.

Adult-born neurons in the hippocampus are positioned mostly in the inner one-third of the GCL[31]. Retrovirus mediated knockdown of ALK5 resulted in a significant delay in migration and an accumulation of DCX+ cells in the SGZ. Constitutive activation of ALK5 on the other hand, led to extended migration of newborn neurons into and beyond the GCL in a reversible fashion. The exact molecular mechanisms that led to this migratory phenotype are unclear but it is intriguing that the microarray analysis identified several gene products with established functions in migration to be differentially expressed between *ALK5*^{CA} and littermate controls mice. In addition, unbiased molecular pathway analysis of the gene array data pointed to “migration of cortical neurons”, “movement”, and JNK signaling. Accordingly, *ALK5*^{CA} mice showed increased expression of three members of the kinesin family and enhanced phosphorylation of JNK. The microtubule-associated protein DCX which stabilizes microtubules[41] is phosphorylated by JNK and associates with the JNK-interacting protein (JIP) and kinesin to mediate neurite outgrowth and neuronal migration[42]. Whether TGF-β signaling promotes newborn neuron migration *in vivo* through phosphorylation of JNK and interaction of DCX and kinesin needs further characterization.

Abnormal migration of newborn neurons has been observed in several developmental disorders caused by mutations in genes, such as *dcx, lis1, and reelin*[43]. In mice, mutations in *disc1*[44] or lack of *girdin*[45] have been shown to cause excessive migration of newborn neurons in the dentate gyrus. Particularly striking is the resemblance of several of the phenotypes observed in *ALK5*^{CA} mice, including hypertrophic cell bodies, accelerated migration and dendritic development of newborn neurons, elevated active newborn neurons, with the phenotypes reported in Disrupted-In-Schizophrenia 1 (DISC1)-knockdown mice[46]. In addition, altered positioning of immature neurons in the GCL of *ALK5*^{CA} mice is also reminiscent of the schizophrenia-like phenotype described in a number of *disc1* mutant mouse models[44]. Haploinsufficiency of the *disc1* gene in humans is a strong risk factor for schizophrenia and the *disc1* gene has been linked to a number of psychiatric phenotypes[47]. It is of interest that TGF-β signaling is hyperactive and ALK5 is significantly upregulated in schizophrenia patients[48]. In light of our current data, it is tempting to speculate that there is a link between injury associated, increased TGF-β signaling, DISC1, and abnormal neuronal migration in the adult hippocampus and that this connection may be relevant to mental illness.

Our findings suggest that TGF-β signaling is an important regulator of the late stages of adult neurogenesis. Because adult neurogenesis has been shown to be important for learning, memory, and mood regulation[49], targeted manipulation of TGF-β signaling in newborn neurons might be useful in regulating these processes in the aged or diseased brain.

Methods

Animals

ALK5 foxed mice (obtained from Stefan Karlsson, Lund University Hospital, Lund, Sweden) have been previous described[50]. To generate *ALK5*^{cKO} mice, homozygous *ALK5* floxed mice were bred with *CamKII*α-*cre* mice on a C57BL/6 genetic background. *mT/mG* mice[26] were obtained from The Jackson Laboratory (Stock No. 007676). Transgenic mice expressing both a constitutively active mutant of ALK5 containing a T204D substitution (ALK5^{CA})[51] fused with HA and eGFP under control of a bi-directional tetO promoter[52] (tetO-*ALK5*^{CA}) were generated using standard procedures. Briefly, the coding sequence of rat *ALK5*^{CA}-HA was isolated from pCMV5-r*ALK5*^{CA}-HA (obtained from Joan Massague, Memorial Sloan-Kettering Cancer Center, New York, NY)[51], subcloned into pBI-EGFP (Clontech), and microinjected into fertilized embryos from FVB mice. TetO-*ALK5*^{CA} mice were homozygous for the *ALK5*^{CA} transgene and on the FVB genetic background. *CamKII*α-*tTA* mice expressing tTA mostly in neurons have been described previously[29] and were crossed with tetO-*ALK5*^{CA} mice to generate double-transgenic *ALK5*^{CA} mice. *ALK5*^{CA} transgenic littermates with only tetO-ALK5^{CA} expression (*ALK5*^{Ctrl} mice), only tTA expression (tTA mice), and wildtype (WT) mice served as control. Only male mice on the FVB genetic background were used throughout the study and except where indicated they were 3-4 months of age. Mice were kept under a 12-hour light/12-hour dark cycle with free access to sterile food and acidified water, 1 to 4 mice per cage. Behavioral tests were assessed during light cycle. Before sacrifice, mice were deeply anesthetized with chloral hydrate, and then flush-perfused transcardially with phosphate buffer. One hemibrain was fixed for 48 hours in 4% paraformaldehyde and equilibrated in 30% sucrose for histological processing. Forty-μm coronal sections were cut using a microtome (Leica Microsystems) with a freezing stage. From the other hemibrain, the hippocampus was dissected, snap-frozen on dry ice, and stored at –80°C until use. All animal care and use was in accordance with institutional guidelines and approved by the Palo Alto VA Committee on Animal Research.

Luciferase activity assay

Brains of SBE-luciferase reporter mice (2-month-old) were dissected into dentate gyrus, CA areas, and cerebellum. Each subregion was lysed in 100-400 μl of cell culture lysis reagent (Promega). Luciferase activities from tissue homogenates were measured and normalized to protein amount assayed by BCA protein assay kit (Pierce).

Viruses

A sequence encoding for cre recombinase was amplified by PCR from pCAG-*cre* plasmid and subcloned into lentiviral vector pFCK(1.3)GW (Addgene plasmid 27230) driving the transgene under *CamKII*α promoter[53]. We designed shRNAs (shRNA-A1 and shRNA-A2)

targeting *ALK5* and control shRNA, which were synthesized (Invitrogen) and subcloned into retroviral vector MSCV-LMP (Open Biosystem) containing an IRES-*eGFP*. *mCherry* retroviral construct was made by replacing eGFP with mCherry. To validate the efficiency of shRNAs, retroviral shRNA vectors and expression constructs for ALK5 were cotransfected into HEK293T cells and cell lysates were prepared for immunoblots. Viruses were produced by the Stanford Neuroscience Gene Vector and Virus Core. Titers were at least 10^7 IU/ml. The target sequences are *AATGGAGATTGTTGGTACCCAA* for shRNA-A1, *AGCTGACAGCTTTGCGAATTAA* for shRNA-A2, and *ATCTCGCTTGGGCGAGAGTAAG* for shRNA-C.

Stereotaxic injections into the dentate gyrus

Adult 2-month-old female C57BL/6 mice wildtype (Jackson Laboratories) or *ALK5*^{flox} mice were anaesthetized and viruses were stereotaxically injected into the dentate gyrus at 4 sites (1 μl per site at 0.25 μl/min) with the following coordinates (posterior = 2.1 mm from Bregma, lateral = ± 1.6 mm, ventral = 2.3 mm; posterior = 3 mm from Bregma, lateral = ± 2.6 mm, ventral = 3.2 mm). C57BL/6 mice were sacrificed 7,14, and 21 days later after retrovirus injection or *ALK5*^{flox} mice were sacrificed 6,14, and 21 days later lentivirus injection. *ALK5*^{flox} mice were given BrdU after lentivirus injection.

Immunohistochemistry

Immunohistochemistry was performed as previously described[54]. 3,3-Diaminobenzidine (Sigma) stains were performed using an ABC labeling kit (Vector Laboratories, Burlingame, CA). Primary antibodies were chosen according to previous studies in our lab or reports in the literature or instructions from the vendors: Rabbit anti-P-Smad2 (1:1000; Chemicon, AB3849), rabbit anti-eGFP (1:500; Life Technologies, A11122), chicken anti-eGFP (1:1000, Avis, GFP-1020), mouse anti-mCherry (1:200, Clontech, 632543), chicken anti-Tbr2 (1:500, Millipore, AB15894), mouse anti-MCM2 (1:500, BD Biosciences, 610700), rat anti-BrdU (1:1000; Abcam, AB6326), goat anti-DCX (1:500; Santa Cruz Biotechnology, sc-8066), mouse anti-PCNA (1:200; DAKO, M0879), rabbit anti-GFAP (1:1000; DAKO, Z0334), mouse anti-NeuN (1:1000; Millipore, MAB377), goat anti-Sox2 (1:200, Santa Cluz Biotechnology, sc-17320), mouse anti-HA (1:1000; Covance, MMS-101P), rabbit anti-c-fos (1:10000; Millipore, PC38). Antigen retrieval with 3 mol/L HCl was used for BrdU. For fluorescent stains, secondary antibodies were purchased from either Molecular Probes or Jackson Immunoresearch. For fluorescent staining procedures, final washes included the nuclear stain Topro-3 (1:500; Molecular Probes) or DAPI (5 μg/mL, Sigma) for 0.5 h at room temperature.

Confocal imaging and somato-dendritic analysis

Fluorescence images were obtained on a confocal-laser microscope (LSM 510 meta Pascal, or LSM710, or LSM 700; Carl Zeiss MicroImaging, Inc.) using a multi-track configuration. For analysis of p-Smad2 cellular signals, a single confocal image slice from a Z-series stack showing the highest p-Smad2 level with or without eGFP expression was chosen and quantified. For analysis of cell morphology *in vivo*, Z-series stacks of confocal images were captured. For analysis of neuronal migration *in vivo*, Z-series stacks of confocal images of

DCX+ cells with Topro-3 staining were taken to determine the localization of DCX+ cells in the GCL. For analysis of soma size of DCX+ immature neurons *in vivo*, a single confocal image slice from a Z-series stack showing the largest soma area was chosen and quantified using the NIH ImageJ software program. For analysis of dendritic complexity *in vivo*, three-dimensional reconstructions of the entire dendritic processes of individual neurons were made from Z-series stacks of confocal images. The projection images were traced and analyzed with NIH ImageJ. Sholl analysis for dendritic complexity was carried out by counting the number of dendrites that crossed a series of concentric circles at 5 μm intervals from the cell soma. For all of the above analyses, a minimum of 6 individual DCX+ immature neurons randomly picked from each mouse from at least 4 mice per group were analyzed.

Microarray analysis

Hippocampi were dissected from hemibrains and total RNA was extracted using Trizol reagent (Invitrogen). cDNA and cRNA were sequentially synthesized and amplified using RNA amplification kit (Ambion) according to the manufacturer's protocol. cRNA was then hybridized to Illumina beadchip array MouseWG-6 (Illumina) according to the manufacturer's instructions. The data were analyzed by Illumina beadstudio data analysis software (Illumina) as described by the manufacturer's guidelines. TreeView and Cluster software was used for the hierarchical clustering of the datasets. A 5% *P*-value was applied as a cut-off. Pathway and function analysis was performed using Ingenuity Pathway Analysis tool (Ingenuity Systems).

Semi-stereological quantification

Immunoreactive cells within the dentate GCL and SGZ were counted in a one-in-twelve series of sections (480 μm apart) throughout the hippocampus. The volume of the GCL in each section was calculated by measuring the Topro-3 region using Metamorph software and multiplying it with the thickness of sections (40 μm). Cell densities in the dentate gyrus were calculated as the number of immunopositive cells divided by the volume of the GCL and expressed as number of immunopositive cells per dentate GCL volume in mm^3. To measure the proportion of colocalized cells, we acquired Z-series stacks of confocal images, examined 100 to 150 BrdU-positive cells from each mouse for each stain and determine whether they co-labeled with DCX, NeuN, or c-fos.

Western blots

Hippocampi dissected from hemi-brains of mice were homogenized and lysed. After centrifugation at 13,000 g, protein concentrations were measured using the BCA protein assay kit (Pierce) and lysates were separated on a 4 to 12% Bis-Tris gels (Invitrogen) using MOPS sodium dodecyl sulfate running buffer (Invitrogen), electroblotted onto PVDF membranes (Millipore), and analyzed with rabbit anti-p-Smad2 (1:1000; Chemicon, AB3849), rabbit anti-Smad2 (1:1000; Cell Signaling Technology, 3102S), mouse anti-HA (1:1000; Covance, MMS-101P), rabbit anti-ALK5 (1:200, Abcam, AB31013), rabbit anti-Bcl-2 (1:1000, Santa Cruz, sc-492), rabbit anti-Bax (1:1000, Santa Cruz, sc-526), mouse anti-NSE (1:1000, Thermo Scientific, AMPA6696) rabbit anti-p-JNK (1:1000, Cell

Signaling Technology, 9251S), rabbit anti-eGFP (1:1000, Life Technologies, A11122), and rabbit anti-actin (1:5000, Sigma, A-5060) antibodies. Signal intensities were detected using ECL Western blotting detection reagents (Amersham Biosciences).

Doxycycline treatment

To confirm that the tetO-*ALK5*^{CA} transgene can be regulated, doxycycline-containing food pellets (doxycycline chow; 625 mg/kg; Teklad) were fed ad libitum to pregnant mice from E17 until postnatal day P56. All pups were then divided into two cohorts. One cohort was maintained on doxycycline food while the other received regular chow for 2 months until all mice were sacrificed. These mice were used for analysis of transgene and DCX expression.

Y maze

The Y-maze was made of solid white plastic and consisted of two symmetrical arms and one longer arm at 120° angles (longer arm, 20.7 cm length × 12.7 cm height × 7.62 cm width; equal arms, 15.24 cm length × 12.7 cm height ×7.62 cm width). Mice were placed in the end of the longer arm and allowed to freely explore the three arms for 5 min. Arm entry was defined as having all four limbs inside an arm. The maze was cleaned with 70% (v/v) ethanol between animals and before the first animal to eliminate traces of odor. The number of arm entries and the number of triads were recorded in order to calculate the alternation percentage, which was calculated by dividing the number of triads by the number of possible alternations multiplied by 100. A triad was defined as a set of consecutive arm entries[55]. Y maze were performed blindly and the data were combined from two independent experiments.

Contextual fear conditioning

Paradigm was done as previously described[56]. Conditioned fear was displayed as freezing behavior. On the first day (training day), mice were placed in the chamber for a 3-min baseline recording followed by five tone-shock pairings with time of 60 sec each pair. The shocks (0.7 mA, 2 sec) were delivered at the end of the tone (70 dB, 2 kHz, 20 sec). On day 2 each mouse was first place in the fear-conditioning chamber containing the same exact context, but with no administration of tone or foot shock. Freezing was analyzed for four minutes. One hour later, the mice were placed in a new context containing a different odor of 3% (v/v) acetic acid, floor texture, and chamber walls and shape. Animals were allowed to explore for 3 minutes before being re-exposed to the tone for another 3 minutes. Freezing was defined as the complete absence of motion including motion of the vibrissae except normal respiration. Freezing was measured using a FreezeScan video tracking system and software (Cleversys, Inc).

Published contextual freezing values differ widely among different studies using FVB mice depending on the supplier of the strain, the detection system, and the training protocols. March et al. showed 0 – 5% freezing[57], Owen et al. reported 13% freezing[58], and Farley et al. reported around 25% freezing[59]. Our mice showed 3 – 6% freezing which is within the above range. The lower freezing behavior of mice on this compared to other backgrounds may be due to a combination of insensitivity of their feet to the electrical shocks and retinal degeneration[59].

Statistical analysis

The distribution of data in each set of experiments was tested for normality using a Kolmogorov-Smirnov test or a Shapiro-Wilk test. The similarity of variances between each group of data was tested using the F test. We carried out pilot studies to estimate sample sizes of final experiments. Data analysis was performed blindly and samples were assigned randomly to groups. We excluded data points that are over 3 standard deviations from the mean in Supplementary Fig. 7c. Differences between two means were assessed by unpaired two-tailed Student's t test. In experiments with stereotaxic injections, differences between two means were assessed by paired two-tailed Student's t test. Differences among multiple means were assessed by one-way ANOVA followed by Tukey's or Dunnett's post-hoc tests. Data from doxycycline treatment experiments were analyzed by two-way ANOVA followed by Sidak's post-hoc test. Data from fear conditioning behavioral experiments were analyzed by two-way repeated-measures ANOVA followed by Bonferroni's post-hoc test. All statistical analyses were performed with GraphPad Prism 5 (GraphPad Software) or SPSS.

Supplementary Material

Refer to Web version on PubMed Central for supplementary material.

Acknowledgements

We thank our lab members for discussions and comments, Dr. Kurt Lucin for editorial assistance, Dr. Jian Luo for comments on data analysis, Gregor Bieri for providing brain sections of *mT/mG* mice crossing with *CamKII*α*-cre* mice, Lian Boerma for helping mouse behavioral tests, Dr. Pavel Osten for providing pFCK(1.3)GW plasmid, and Michael Lochrie and the Stanford Neuroscience Gene Vector and Virus Core for generating the viruses (supported by NINDS P30 core grant, NS069375-01A1). This work was supported by NIH grant AG27505 (T.W.-C.) and the Department of Veterans Affairs (T.W.-C.). Authors have no financial interest related to this work.

References

1. Krieglstein K, Zheng F, Unsicker K, Alzheimer C. More than being protective: functional roles for TGF-beta/activin signaling pathways at central synapses. Trends Neurosci. 2011; 34:421–429. [PubMed: 21742388]
2. Blobe GC, Schiemann WP, Lodish HF. Role of transforming growth factor beta in human disease. N Engl J Med. 2000; 342:1350–1358. [PubMed: 10793168]
3. Unsicker K, Flanders KC, Cissel DS, Lafyatis R, Sporn MB. Transforming growth factor beta isoforms in the adult rat central and peripheral nervous system. Neuroscience. 1991; 44:613–625. [PubMed: 1754055]
4. Shi Y, Massague J. Mechanisms of TGF-beta signaling from cell membrane to the nucleus. Cell. 2003; 113:685–700. [PubMed: 12809600]
5. Feng XH, Derynck R. Specificity and Versatility in TGF-Signaling Through Smads. Annu Rev Cell Dev Biol. 2005
6. Tomoda T, et al. Transforming growth factor-beta is a survival factor for neonate cortical neurons: coincident expression of type I receptors in developing cerebral cortices. Dev Biol. 1996; 179:79–90. [PubMed: 8873755]
7. Falk S, et al. Brain area-specific effect of TGF-beta signaling on Wnt-dependent neural stem cell expansion. Cell Stem Cell. 2008; 2:472–483. [PubMed: 18462697]
8. Ishihara A, Saito H, Abe K. Transforming growth factor-beta 1 and -beta 2 promote neurite sprouting and elongation of cultured rat hippocampal neurons. Brain Res. 1994; 639:21–25. [PubMed: 8180834]

9. Ng J. TGF-beta signals regulate axonal development through distinct Smad-independent mechanisms. Development. 2008; 135:4025–4035. [PubMed: 19004854]
10. Yi JJ, Barnes AP, Hand R, Polleux F, Ehlers MD. TGF-beta signaling specifies axons during brain development. Cell. 2010; 142:144–157. [PubMed: 20603020]
11. Unsicker K, Krieglstein K. TGF-betas and their roles in the regulation of neuron survival. Adv Exp Med Biol. 2002; 513:353–374. [PubMed: 12575828]
12. Tesseur I, Wyss-Coray T. A role for TGF-beta signaling in neurodegeneration: evidence from genetically engineered models. Curr Alzheimer Res. 2006; 3:505–513. [PubMed: 17168649]
13. Brionne TC, Tesseur I, Masliah E, Wyss-Coray T. Loss of TGF-beta1 leads to increased neuronal cell death and microgliosis in mouse brain. Neuron. 2003; 40:1133–1145. [PubMed: 14687548]
14. Tesseur I, et al. Deficiency in neuronal TGF-beta signaling promotes neurodegeneration and Alzheimer's pathology. J Clin Invest. 2006; 116:3060–3069. [PubMed: 17080199]
15. Buckwalter MS, et al. Chronically increased transforming growth factor-beta1 strongly inhibits hippocampal neurogenesis in aged mice. Am J Pathol. 2006; 169:154–164. [PubMed: 16816369]
16. Wachs FP, et al. Transforming growth factor-beta1 is a negative modulator of adult neurogenesis. J Neuropathol Exp Neurol. 2006; 65:358–370. [PubMed: 16691117]
17. Deng W, Aimone JB, Gage FH. New neurons and new memories: how does adult hippocampal neurogenesis affect learning and memory? Nat Rev Neurosci. 2010; 11:339–350. [PubMed: 20354534]
18. Faigle R, Song H. Signaling mechanisms regulating adult neural stem cells and neurogenesis. Biochim Biophys Acta. 2012
19. Parent JM. Injury-induced neurogenesis in the adult mammalian brain. Neuroscientist. 2003; 9:261–272. [PubMed: 12934709]
20. Duan X, Kang E, Liu CY, Ming GL, Song H. Development of neural stem cell in the adult brain. Curr Opin Neurobiol. 2008; 18:108–115. [PubMed: 18514504]
21. Luo J, Lin AH, Masliah E, Wyss-Coray T. Bioluminescence imaging of Smad signaling in living mice shows correlation with excitotoxic neurodegeneration. Proc Natl Acad Sci U S A. 2006; 103:18326–18331. [PubMed: 17110447]
22. Lin AH, et al. Global analysis of Smad2/3-dependent TGF-beta signaling in living mice reveals prominent tissue-specific responses to injury. J Immunol. 2005; 175:547–554. [PubMed: 15972691]
23. Plumpe T, et al. Variability of doublecortin-associated dendrite maturation in adult hippocampal neurogenesis is independent of the regulation of precursor cell proliferation. BMC Neurosci. 2006; 7:77. [PubMed: 17105671]
24. Mazerbourg S, Hsueh AJ. Genomic analyses facilitate identification of receptors and signalling pathways for growth differentiation factor 9 and related orphan bone morphogenetic protein/growth differentiation factor ligands. Hum Reprod Update. 2006; 12:373–383. [PubMed: 16603567]
25. Wu HH, et al. Autoregulation of neurogenesis by GDF11. Neuron. 2003; 37:197–207. [PubMed: 12546816]
26. Muzumdar MD, Tasic B, Miyamichi K, Li L, Luo L. A global double-fluorescent Cre reporter mouse. Genesis. 2007; 45:593–605. [PubMed: 17868096]
27. Marxreiter F, et al. Changes in adult olfactory bulb neurogenesis in mice expressing the A30P mutant form of alpha-synuclein. Eur J Neurosci. 2009; 29:879–890. [PubMed: 19291219]
28. Imielski Y, et al. Regrowing the adult brain: NF-kappaB controls functional circuit formation and tissue homeostasis in the dentate gyrus. PLoS One. 2012; 7:e30838. [PubMed: 22312433]
29. Mayford M, et al. Control of memory formation through regulated expression of a CaMKII transgene. Science. 1996; 274:1678–1683. [PubMed: 8939850]
30. Jessberger S, Romer B, Babu H, Kempermann G. Seizures induce proliferation and dispersion of doublecortin-positive hippocampal progenitor cells. Exp Neurol. 2005; 196:342–351. [PubMed: 16168988]

31. Kempermann G, Gast D, Kronenberg G, Yamaguchi M, Gage FH. Early determination and long-term persistence of adult-generated new neurons in the hippocampus of mice. Development. 2003; 130:391–399. [PubMed: 12466205]
32. Stevens B, et al. The classical complement cascade mediates CNS synapse elimination. Cell. 2007; 131:1164–1178. [PubMed: 18083105]
33. Hevner RF, et al. Tbr1 regulates differentiation of the preplate and layer 6. Neuron. 2001; 29:353–366. [PubMed: 11239428]
34. Bury FJ, et al. Xenopus BTBD6 and its Drosophila homologue lute are required for neuronal development. Dev Dyn. 2008; 237:3352–3360. [PubMed: 18855900]
35. Resende RR, da Costa JL, Kihara AH, Adhikari A, Lorencon E. Intracellular Ca2+ regulation during neuronal differentiation of murine embryonal carcinoma and mesenchymal stem cells. Stem Cells Dev. 2010; 19:379–394. [PubMed: 19032055]
36. Hirokawa N, Noda Y, Tanaka Y, Niwa S. Kinesin superfamily motor proteins and intracellular transport. Nat Rev Mol Cell Biol. 2009; 10:682–696. [PubMed: 19773780]
37. Guzowski JF, et al. Mapping behaviorally relevant neural circuits with immediate-early gene expression. Curr Opin Neurobiol. 2005; 15:599–606. [PubMed: 16150584]
38. Park SM, Jung JS, Jang MS, Kang KS, Kang SK. Transforming growth factor-beta1 regulates the fate of cultured spinal cord-derived neural progenitor cells. Cell Prolif. 2008; 41:248–264. [PubMed: 18336470]
39. Prehn JH, et al. Regulation of neuronal Bcl2 protein expression and calcium homeostasis by transforming growth factor type beta confers wide-ranging protection on rat hippocampal neurons. Proc Natl Acad Sci U S A. 1994; 91:12599–12603. [PubMed: 7809085]
40. Krieglstein K, Suter-Crazzolara C, Fischer WH, Unsicker K. TGF-beta superfamily members promote survival of midbrain dopaminergic neurons and protect them against MPP+ toxicity. EMBO J. 1995; 14:736–742. [PubMed: 7882977]
41. Gleeson JG, Lin PT, Flanagan LA, Walsh CA. Doublecortin is a microtubule-associated protein and is expressed widely by migrating neurons. Neuron. 1999; 23:257–271. [PubMed: 10399933]
42. Gdalyahu A, et al. DCX, a new mediator of the JNK pathway. EMBO J. 2004; 23:823–832. [PubMed: 14765123]
43. Feng Y, Walsh CA. Protein-protein interactions, cytoskeletal regulation and neuronal migration. Nat Rev Neurosci. 2001; 2:408–416. [PubMed: 11389474]
44. Kvajo M, et al. A mutation in mouse Disc1 that models a schizophrenia risk allele leads to specific alterations in neuronal architecture and cognition. Proc Natl Acad Sci U S A. 2008; 105:7076–7081. [PubMed: 18458327]
45. Enomoto A, et al. Roles of disrupted-in-schizophrenia 1-interacting protein girdin in postnatal development of the dentate gyrus. Neuron. 2009; 63:774–787. [PubMed: 19778507]
46. Duan X, et al. Disrupted-In-Schizophrenia 1 regulates integration of newly generated neurons in the adult brain. Cell. 2007; 130:1146–1158. [PubMed: 17825401]
47. Porteous DJ, Thomson P, Brandon NJ, Millar JK. The genetics and biology of DISC1--an emerging role in psychosis and cognition. Biol Psychiatry. 2006; 60:123–131. [PubMed: 16843095]
48. Benes FM, et al. Regulation of the GABA cell phenotype in hippocampus of schizophrenics and bipolars. Proc Natl Acad Sci U S A. 2007; 104:10164–10169. [PubMed: 17553960]
49. Marin-Burgin A, Schinder AF. Requirement of adult-born neurons for hippocampus-dependent learning. Behav Brain Res. 2012; 227:391–399. [PubMed: 21763727]
50. Larsson J, et al. Abnormal angiogenesis but intact hematopoietic potential in TGF-beta type I receptor-deficient mice. EMBO J. 2001; 20:1663–1673. [PubMed: 11285230]
51. Wieser R, Wrana JL, Massague J. GS domain mutations that constitutively activate T beta R-I, the downstream signaling component in the TGF-beta receptor complex. EMBO J. 1995; 14:2199–2208. [PubMed: 7774578]
52. Gossen M, Bujard H. Tight control of gene expression in mammalian cells by tetracycline-responsive promoters. Proc Natl Acad Sci U S A. 1992; 89:5547–5551. [PubMed: 1319065]

53. Dittgen T, et al. Lentivirus-based genetic manipulations of cortical neurons and their optical and electrophysiological monitoring in vivo. Proc Natl Acad Sci U S A. 2004; 101:18206–18211. [PubMed: 15608064]

54. Mosher KI, et al. Neural progenitor cells regulate microglia functions and activity. Nat Neurosci. 2012; 15:1485–1487. [PubMed: 23086334]

55. Hughes RN. The value of spontaneous alternation behavior (SAB) as a test of retention in pharmacological investigations of memory. Neurosci Biobehav Rev. 2004; 28:497–505. [PubMed: 15465137]

56. Villeda SA, et al. The ageing systemic milieu negatively regulates neurogenesis and cognitive function. Nature. 2011; 477:90–94. [PubMed: 21886162]

57. March A, Borchelt D, Golde T, Janus C. Differences in memory development among C57BL/6NCrl, 129S2/SvPasCrl, and FVB/NCrl mice after delay and trace fear conditioning. Comp Med. 2014; 64:4–12. [PubMed: 24672832]

58. Owen EH, Logue SF, Rasmussen DL, Wehner JM. Assessment of learning by the Morris water task and fear conditioning in inbred mouse strains and F1 hybrids: implications of genetic background for single gene mutations and quantitative trait loci analyses. Neuroscience. 1997; 80:1087–1099. [PubMed: 9284062]

59. Farley SJ, McKay BM, Disterhoft JF, Weiss C. Reevaluating hippocampus-dependent learning in FVB/N mice. Behav Neurosci. 2011; 125:871–878. [PubMed: 22122148]

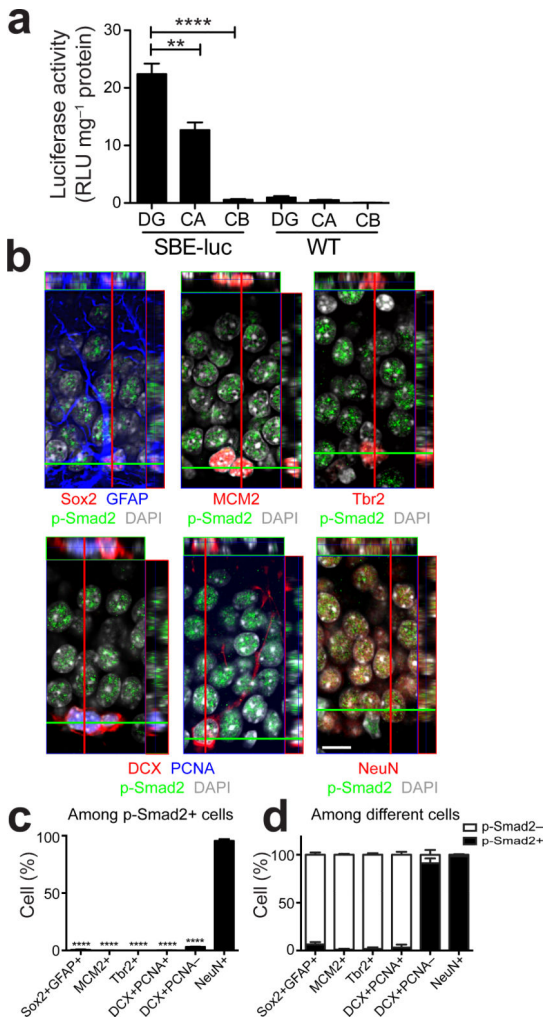

Figure 1.

Physiological TGF-β signaling is active in postmitotic immature and mature neurons of the adult dentate gyrus. (a) Luciferase activity is the highest in the dentate gyrus of the brain of 2-month-old SBE-luciferase reporter mice (n = 3 mice per group). DG, dentate gyrus; CA, cornu ammonis; CB, cerebellum; luc, luciferase. (b) Representative orthogonal projections from confocal Z-stack images of the dentate gyrus from 2-month-old FVB mice immunostained for p-Smad2 in combination with Sox2 plus GFAP, MCM2, Tbr2, DCX plus PCNA, and NeuN. DAPI stains nuclei. Scale bar, 10 μm. (c) Quantification of p-Smad2 positive cells in different cell types detected in (b) from the dentate gyrus of 2-month-old FVB mice. (d) Quantification of p-Smad2 positive and negative cells in individual cell types detected in (b) from the dentate gyrus of 2-month-old FVB mice. n = 4 mice, 3 sections per mouse in (c,d). Data are presented as mean + s.e.m. $^{**}P < 0.01$, $^{****}P < 0.0001$, one-way ANOVA, Tukey's post-hoc test in (a) and Dunnett's post-hoc test in (c).

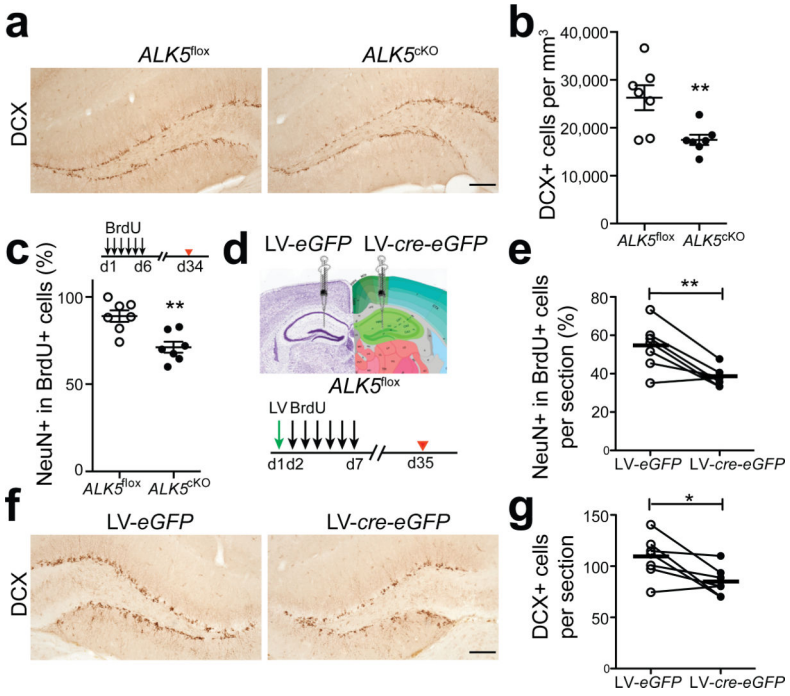

Figure 2.

Ablation of ALK5 results in fewer newborn neurons in the dentate gyrus. (a,b) Immunohistochemical detection (a) and quantification (b) of DCX labeled cells in the dentate gyrus from 3-month-old *ALK5*^{flox} and *ALK5*^{cKO} mice (n = 7 mice per group, 5 sections per mouse, $P = 0.0086$). (c) Quantification of the percentage of BrdU and NeuN double-labeled cells in the dentate gyrus from 3-month-old *ALK5*^{flox} and *ALK5*^{cKO} mice after long-term BrdU labeling (n = 7 mice per group, 5 sections per mouse, $P = 0.0022$). Experimental design inserted on top. (d) Experimental design for the stereotaxic injection of lentivirus into the left or right dentate gyrus of *ALK5*^{flox} mice at the age of 2 months and the long-term BrdU-labeling paradigm. LV, lentivirus. (e) Quantification of BrdU and NeuN double-labeled newborn neurons in the dentate gyrus from stereotaxically injected mice (n = 7 mice, 4 sections per mouse, $P = 0.0059$). (f,g) Immunohistochemical detection (f) and quantification (g) of DCX labeled neurons in the dentate gyrus from stereotaxically injected mice (n = 7 mice, 4 sections per mouse, $P = 0.0306$). Scale bar is 100 μm (a,f). Data are presented as mean ± s.e.m. Connected dots and circles in (e, g) represent left and right dentate gyrus of individual mice, bars in (e,g) represent mean values. *$P < 0.05$, **$P < 0.01$, Student's t-test (b,c); paired t-test (e,g).

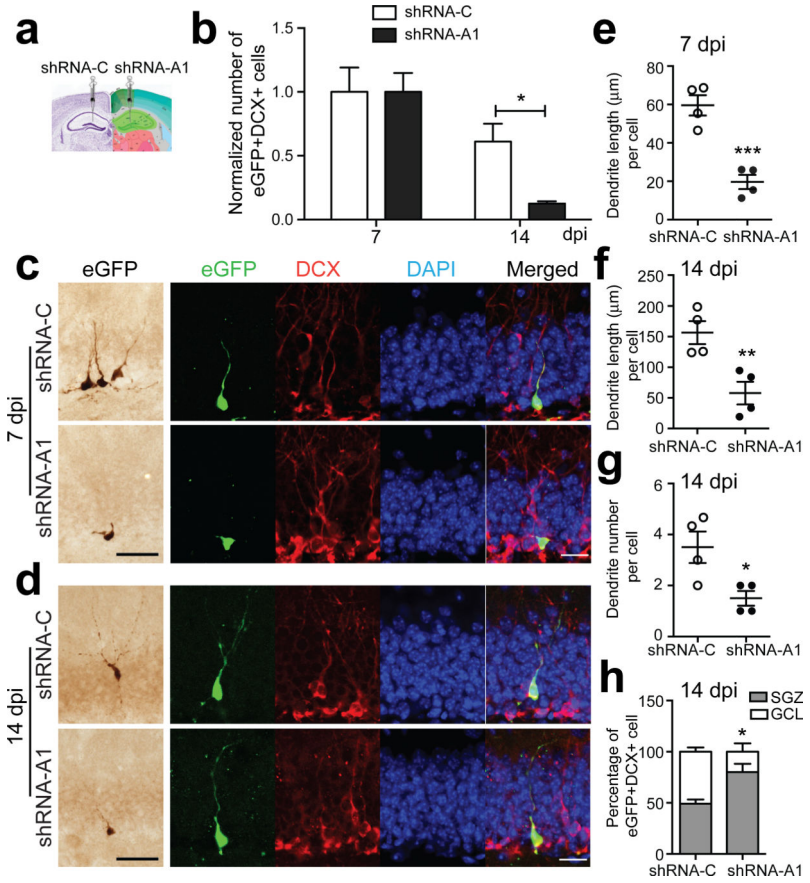

Figure 3.

Loss of ALK5 in progenitor cells affects the survival and morphological maturation of newborn neurons in the dentate gyrus. (a) Experimental design for the stereotaxic injection of retrovirus into the left or right dentate gyrus of 2-month-old female C57BL/6 mice. (b) Quantification of the number of virus-infected eGFP and DCX double-labeled newborn neurons in the dentate gyrus from stereotaxically injected mice at 7 and 14 dpi. Cell numbers were normalized to values at 7 dpi. n = 4 mice per group, 4 sections per mouse, $P = 0.0137$. (c,d) Immunohistochemical detection of virus-infected eGFP labeled cells (left) and confocal images of eGFP, DCX and DAPI triple-labeled newborn neurons (right) in the dentate gyrus at 7 (c) and 14 dpi (d). Scale bar is 50 μm in bright-field microscopy images and 20 μm in confocal images. (e,f) Quantification of dendritic length of virus-infected newborn neurons in the dentate gyrus at 7 (e) and 14 dpi (f). (g,h) Quantification of dendrite number (g) and distribution (h) of virus-infected newborn neurons in the dentate gyrus at 14 dpi. n = 4 mice per group. Data are presented as mean ± s.e.m. $*P < 0.05$, $**P < 0.01$, $***P < 0.001$, Student's t-test.

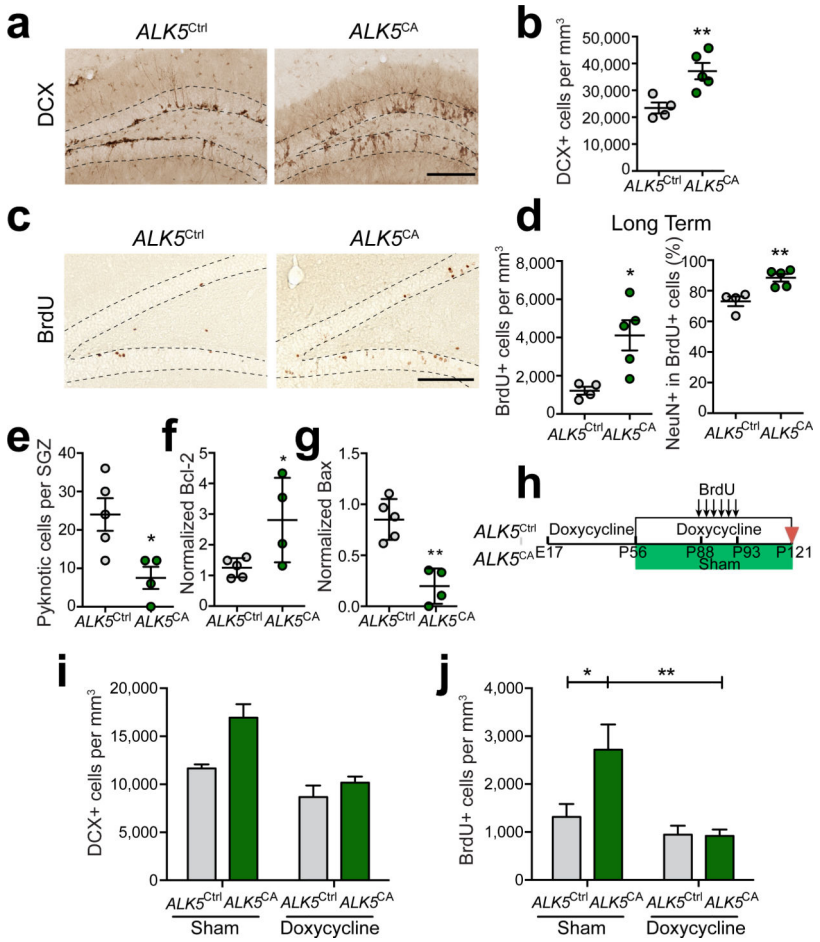

Figure 4.

Overexpression of constitutively active ALK5 leads to an increase in the number of newborn neurons in the dentate gyrus. (a,b) Immunohistochemical detection (a) and quantification (b) of DCX labeled neurons in the dentate gyrus (dotted line) from 3-month-old *ALK5*^{Ctrl} (n = 4) and *ALK5*^{CA} (n = 5) mice (5 sections per mouse, $P = 0.0097$). (c,d) Immunohistochemical detection (c) and quantification (d) of BrdU labeled cells ($P = 0.0159$), as well as quantification of BrdU and NeuN double-labeled newborn neurons ($P = 0.0059$) in the dentate gyrus (dotted line) from 3-month-old *ALK5*^{Ctrl} (n = 4) and *ALK5*^{CA} (n = 5) mice 28 days after BrdU administration. Five sections per mouse. (e) Quantification of the number of pyknotic cells in the SGZ of 3-month-old *ALK5*^{Ctrl} (n = 5) and *ALK5*^{CA} (n = 4) mice (10 sections per mouse, $P = 0.0189$). (f,g) Quantification of Bcl-2 (f) and Bax (g) signal intensity normalized against neuron-specific enolase (NSE) from immunoblots of hippocampal lysates from 3-month-old *ALK5*^{Ctrl} (n = 5) and *ALK5*^{CA} (n = 4) mice. (h) Experimental design for the doxycycline treatment of *ALK5*^{Ctrl} and *ALK5*^{CA} mice. (i,j) Quantification of DCX (i) and BrdU (j) labeled newborn neurons in the dentate gyrus of 4-month-old *ALK5*^{Ctrl} and *ALK5*^{CA} mice before and after treatment with doxycycline (n = 4 mice per group, 5 sections per mouse). In (i), doxycycline × genotype interaction $F(1,12) = 3.598$, $P = 0.0822$; doxycycline treatment $F(1,12) = 23.82$, $P = 0.0004$; genotype $F(1,12) = 11.47$, $P = 0.0054$. In (j), doxycycline × genotype interaction $F(1,12) = 5.099$, $P = 0.0434$;

doxycycline treatment $F(1,12) = 11.73$, $P = 0.0050$; genotype $F(1,12) = 4.714$, $P = 0.0507$. Data are presented as mean ± s.e.m. in (b,d,e,i,j), mean ± s.d in (f,g). *$P < 0.05$, **$P < 0.01$, Student's t-test in (b,d,e-g). Two-way ANOVA in (i,j), Sidak's post-hoc test in (j). Scale bar, 100 μm.

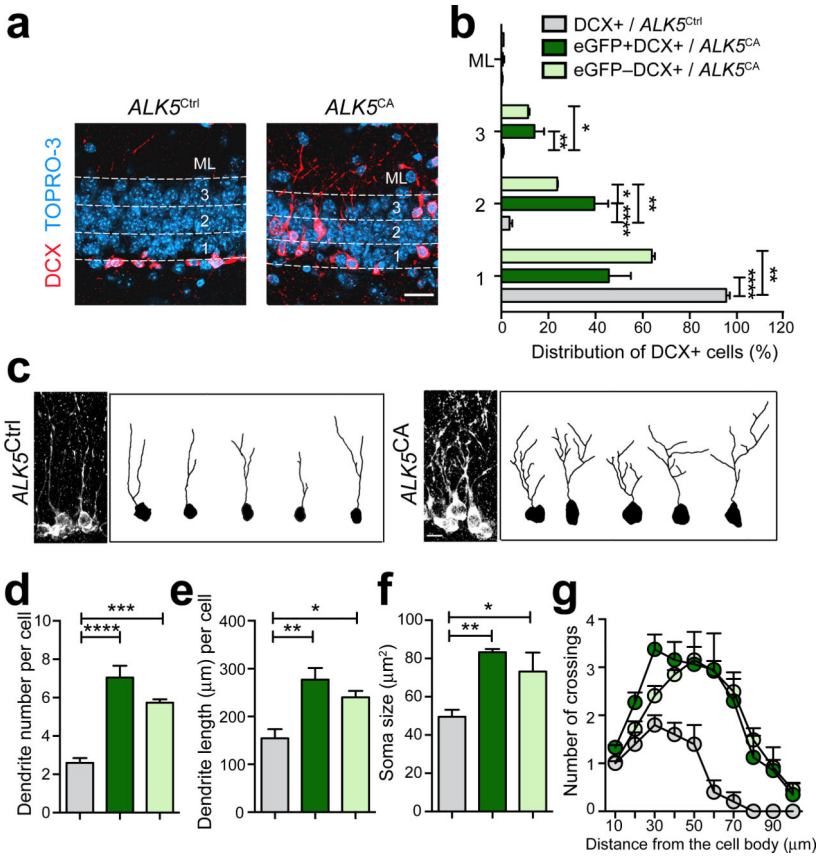

Figure 5.

Overexpression of constitutively active ALK5 accelerates migration and dendritic development of newborn neurons in the adult dentate gyrus. (a) Confocal images of the dentate gyrus of 3-month-old *ALK5*^{Ctrl} and *ALK5*^{CA} mice immunostained for DCX in combination with the nuclear label Topro-3. Numbers 1, 2, 3 label three even layers separated by dotted lines in the GCL. ML, molecular layer. (b) Relative distribution of DCX labeled cells in *ALK5*^{Ctrl} mice and DCX labeled cells with (eGFP+) or without (eGFP–) transgene expression in *ALK5*^{CA} mice in the ML and three different layers of the dentate gyrus, as indicated in (a). (c) 3D confocal reconstruction of dendrites of DCX labeled cells. Example projections of Z-series confocal images of DCX labeled cells from *ALK5*^{Ctrl} and *ALK5*^{CA} mice are shown on the left. Example images of 2D projection trajectories of 3D confocal reconstructions of cell bodies and dendrites of DCX labeled cells are shown on the right. (d-g) Quantification of dendritic number (d), dendritic length (e), soma size (f), and dendritic complexity by Sholl analysis (g) of DCX labeled cells from *ALK5*^{Ctrl} mice and DCX labeled cells with (eGFP+) or without (eGFP–) transgene expression in *ALK5*^{CA} mice. Labels are the same as in (b). Scale bar is 25 µm in (a) and 10 µm in (c). Data are from 5 mice (3-month-old) per group. Data are presented as mean + s.e.m. **P* < 0.05, ***P* < 0.01, ****P* < 0.001, *****P* < 0.0001, one-way ANOVA, Tukey's post-hoc test.

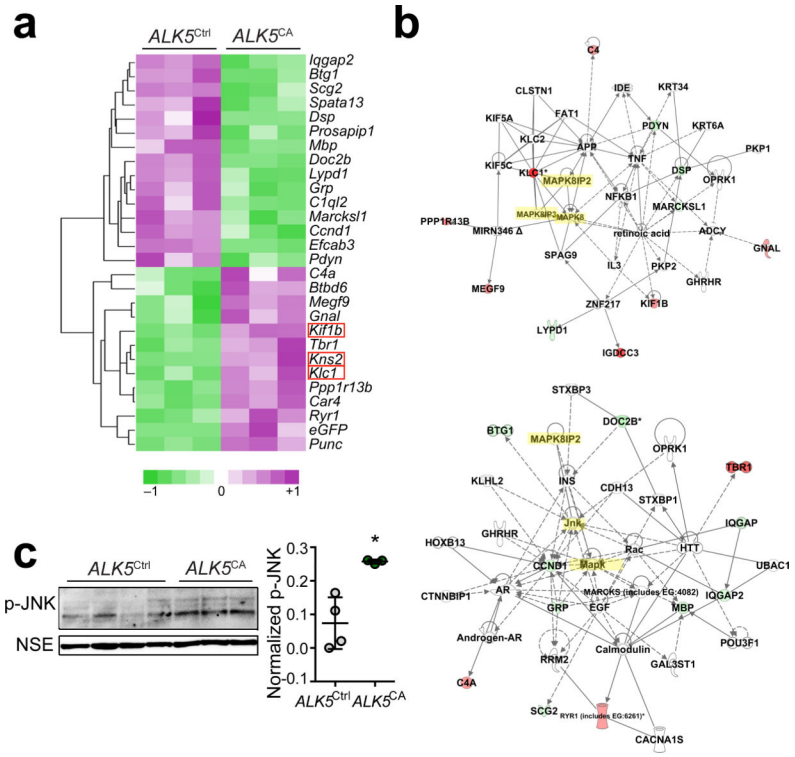

Figure 6.

Overexpression of constitutively active ALK5 results in the expression of hippocampal genes involved in JNK signaling. (a) Heat map generated by clustering with 28 genes differentially expressed between hippocampi of 3-month-old *ALK5*^{Ctrl} and *ALK5*^{CA} mice (n=3 mice per group) analyzed with Illumina beadstudio software. Downregulated genes are shown in shades of green and upregulated genes are shown in shades of purple. Three kinesin family members are highlighted in red boxes. (b) Identification of differentially regulated biological pathways by Ingenuity Pathway Analysis software based on the differentially expressed genes in *ALK5*^{CA} compared with *ALK5*^{Ctrl} mice. Downregulated genes are shown in green and upregulated genes are shown in red. JNK and JIPs are highlighted in yellow. (c) Immunoblot analysis of hippocampal lysates from 3-month-old *ALK5*^{Ctrl} (n = 4) and *ALK5*^{CA} (n = 3) mice probed with antibodies against p-JNK and NSE and quantification of p-JNK signal intensity normalized against NSE. Full-length blots are presented in Supplementary Figure 10. Data are presented as mean + s.d. **P* = 0.0102, Student's t-test.

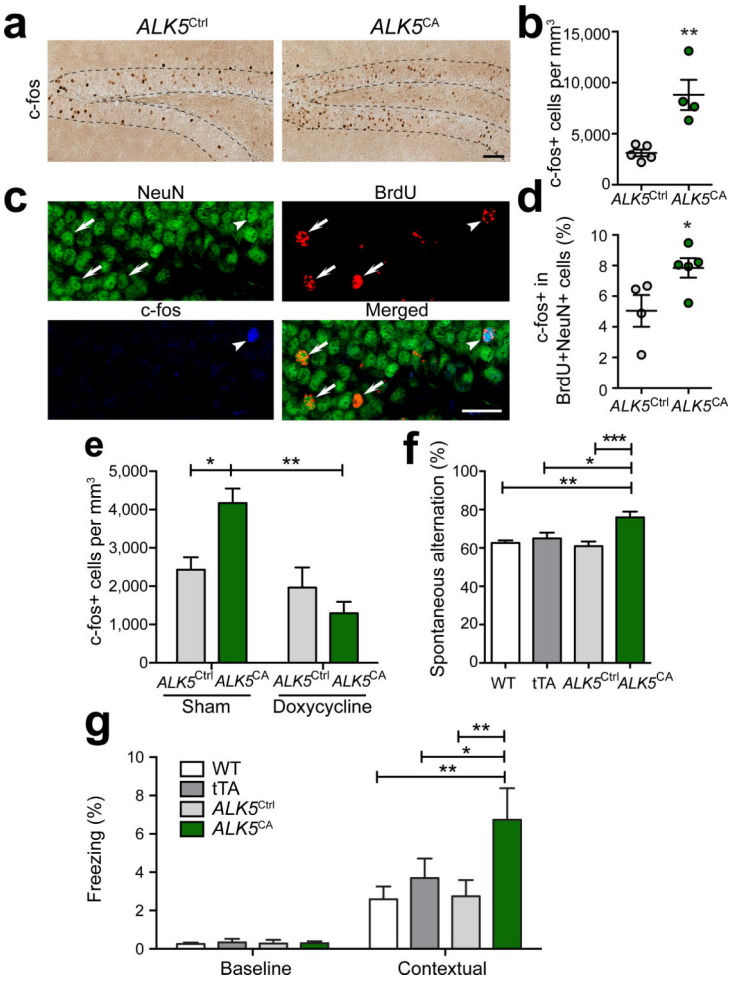

Figure 7.

Overexpression of constitutively active ALK5 enhances activity of newborn neurons in the dentate gyrus and improves memory of *ALK5*^{CA} mice. (a,b) Immunohistochemical detection (a) and quantification (b) of c-fos labeled cells in the dentate gyrus from 3-month-old *ALK5*^{Ctrl} (n = 5) and *ALK5*^{CA} (n = 4) mice (5 sections per mouse, $P = 0.0041$). (c,d) Representative confocal images (c) and quantification (d) of BrdU, NeuN, and c-fos triple-labeled newborn neurons in the dentate gyrus from 3-month-old *ALK5*^{Ctrl} (n = 4) and *ALK5*^{CA} (n = 5) mice (10 sections per mouse, $P = 0.0464$). Arrow identifies BrdU and NeuN double-labeled newborn neurons. Arrowhead indicates BrdU, NeuN, and c-fos triple-labeled newborn neurons. (e) Quantification of c-fos labeled neurons in the dentate gyrus of 4-month-old *ALK5*^{Ctrl} and *ALK5*^{CA} mice before and after doxycycline treatment (n = 4 mice per group, 5 sections per mouse). Doxycycline × genotype interaction $F(1,12) = 9.463$, $P = 0.0096$; doxycycline treatment $F(1,12) = 18.25$, $P = 0.0011$; genotype $F(1,12) = 1.847$, $P = 0.1991$. (f) Percentage of spontaneous alternations in the Y maze was measured in 3-month-old male WT, tTA, *ALK5*^{Ctrl} and *ALK5*^{CA} mice. n = 18 mice per group. (g) Fear conditioning assessed by the percentage of freezing displayed by 3-month-old male WT, tTA, *ALK5*^{Ctrl}, and *ALK5*^{CA} mice under basal condition and re-exposed 24 hours later to the contextual environment after conditioning; n = 11 mice per group. Time × genotype

interaction $F(3,40) = 2.995$, $P = 0.0420$; time $F(1,40) = 43.28$, $P < 0.0001$; genotype $F(3,40) = 2.982$, $P = 0.0426$. Scale bar is 100 μm in (a) and 25 μm in (c). Data are presented as mean + s.e.m. * $P < 0.05$, ** $P < 0.01$, *** $P < 0.001$, Student's t-test (b,d); Two-way ANOVA, Sidak's post-hoc test (e); one-way ANOVA, Tukey's post-hoc test (f); Two-way repeated-measures ANOVA, Bonferroni's post-hoc test (g).